Imaging of Current Density within a Planar Specimen

Patrick A. Hölzl and Bernhard G. Zagar
Johannes Kepler University of Linz,
Altenbergerstr. 69, 4040 Linz, Austria
patrick.hoelzl@jku.at, bernhard.zagar@jku.at

***Abstract*—Magnetic imaging is an non–destructive testing (NDT) method which leads to an inverse problem if the underlying current density should be determined. The current density permits either the determination of the geometry or the conductivity of an electrical conductor. For analyzing novel electrically conductive materials, the uniformity of the conductivity is a critical characteristic. This paper presents a deconvolution based method to determine the current density distribution within an inhomogeneous electrical conductor from the resulting magnetic field measured with a state of the art GMR magnetometer.**

***Index Terms*—Conductivity measurement, Deconvolution, Inverse problems, Magnetometer**

I. Introduction

The methodology to determine a not directly observable parameter via a measurable physical quantity is known as solving an inverse problem. An inverse problem arises when the current density within an electrical conductor should be determined via the resulting magnetic field. Using the current density, characteristics of a conductor such as its geometry or its conductivity can be determined. The conductivity is an important parameter for analyzing novel electrically conductive materials, which allows to draw conclusions about the homogeneity of the material. This paper presents a deconvolution based method to determine the current density within an inhomogeneous and anisotropic electrically conductive material from the magnetic field measured by a GMR magnetometer. Furthermore, a deconvolution based procedure to improve the spatial resolution of the used magnetic field sensor is presented.

II. Problem Description

Fig. 1 shows a schematic of the specimen consisting of 28 strands (each with a triangular cross–section) which extend in x–direction. Due to the manufacturing process and the material composition, the conductivity κ of the specimen is inhomogeneous.

Based on Ohm's law $\vec{J}=\kappa\vec{E}$ and the continuity equation $\nabla\cdot\vec{J}=0$, the current density $\vec{J}$ inside the specimen is deflected by spatially varying conductivity $\kappa(x',y',z')$, where x',y',z' are coordinates located inside the specimen volume V'. Since the law of Biot–Savart (1) couples magnetic fields and spatial current density distributions, variations of κ are recognizable by measuring the magnetic field.

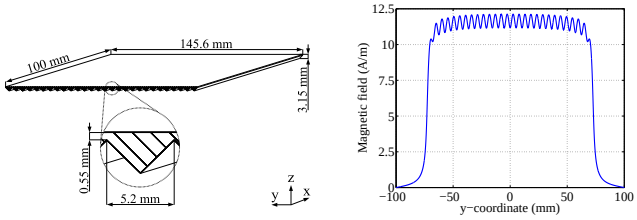

Figure 1. The right image shows a schematic of the specimen. The left image shows the field component $H_y(x_0,y)$, $0.6\ \mathrm{mm}$ above a homogeneous specimen obtained from COMSOL.

$$\begin{pmatrix}H_x\\H_y\\H_z\end{pmatrix}=\frac{1}{4\pi}\int\frac{(J_x,J_y,J_z)^T\times(x-x',y-y',z-z')^T}{((x-x')^2+(y-y')^2+(z-z')^2)^{3/2}}\,\mathrm{d}V' \quad (1)$$

Fig. 1 shows the magnetic field component $H_y(x_0,y)$ along the y–direction for a specimen with homogeneous conductivity obtained by FEM simulation. In agreement with the measurement setup the field component was simulated for a constant current of 3.482 A in negative x–direction, $0.6\ \mathrm{mm}$ above the specimen.

III. Measurement Results

The magnetic field component $H_y(x,y)$ was measured using a NVE AA005–02 magnetometer. The magnetometer output voltage is proportional to the magnitude of the magnetic field component along its sensitive axis. A 3–axis precision translation stage was used for spatial sampling of the magnetic field in increments of $\Delta x{=}2\ \mathrm{mm}$ and $\Delta y{=}0.5\ \mathrm{mm}$, while a constant current of 3.482 A was applied to the specimen in negative x–direction. Fig. 2 shows the measured field component $\widetilde{H}_y(x,y)$, $0.6\ \mathrm{mm}$ above the specimen. At $x{=}{-}5\ \mathrm{mm}$

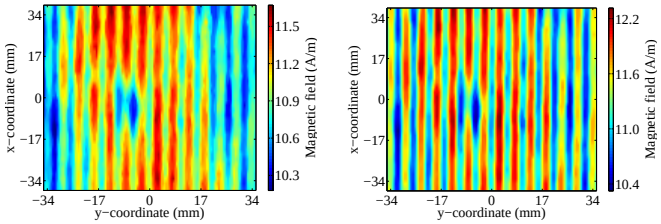

Figure 2. Measured field component $\widetilde{H}_y(x,y)$ (left side) and estimated original field component $\widehat{H}_y(x,y)$ (right side) obtained via a deconvolution.

and $y{=}{-}14\ \mathrm{mm}$ a small field inhomogeneity is visible. The measured field is smaller and spatially smoother than the FEM

results in Fig. 1. The inherent spatial low–pass filtering arises from the sensors flux concentrators. In order to reverse the impact of the internal structure, the sensor is modeled in (2) as a linear space–invariant (LSI) system.

$$\widetilde{H}_y(x,y) = H_y(x,y) * G(x,y) + N(x,y) \tag{2}$$

$\widetilde{H}_y(x,y)$ is the measured (distorted) field, $H_y(x,y)$ is the original field, $N(x,y)$ is additive noise and $G(x,y)$ is the sensitivity function aka. point spread function (PSF) of the sensor [1]. To determine $H_y(x,y)$, the convolution must be reversed taking into account $N(x,y)$, this process is called deconvolution [2]. The sensors PSF can be determined by deconvolving the measured field above a rectangular conductor with its analytical solution via a Wiener filter [3]. Based on the PSF an estimate of the original field $\widehat{H}_y(x,y)$ was computed from $\widetilde{H}_y(x,y)$ using a Wiener filter, see Fig. 2. The overall distribution of $\widehat{H}_y(x,y)$ agrees significantly better with the FEM results.

IV. Solving The Inverse Problem

According to [4], the field component $H_y(x,y)$ at the distance z resulting from a current density component $J_x(x,y)$ within a thin 2D structure of thickness d can be expressed by

$$H_y(x,y) = \frac{zd}{4\pi} \iint \frac{-J_x(x',y')}{((x-x')^2 + (y-y')^2 + z^2)^{3/2}} \, \mathrm{d}x'\mathrm{d}y', \tag{3}$$

which is derived from (1) or by an equivalent convolution

$$H_y(x,y) = -J_x(x,y) * G_{\mathrm{Biot}}(x,y). \tag{4}$$

Equation (4) represents an inverse problem that can be solved by deconvolution. Fig. 3 shows the current density component $\widetilde{J}_x(x,y)$ computed from $\widehat{H}_y(x,y)$ (see Fig. 2) via a deconvolution, using the Lucy–Richardson algorithm. Experiments with other samples [5] have shown that the Lucy–Richardson algorithm provides better results than a Wiener or a regularized filter for the computation of $\widetilde{J}_x(x,y)$.

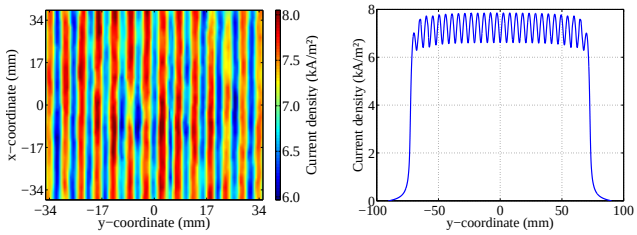

Figure 3. The left image shows $\widetilde{J}_x(x,y)$ obtained via deconvolving $\widehat{H}_y(x,y)$ with the Biot–Savart filter function $G_{\mathrm{Biot}}(x,y)$. The right image shows $\widetilde{J}_x(x_0,y)$ computed similarly from the FEM results with $G_{\mathrm{Biot}}(x_0,y)$.

In contrast to the assumptions ($z - z' \approx z$; $\mathrm{d}z' = d$; $J_z \ll J_x$; $J_z \ll J_y$) made to derive (3) from (1), the specimen possesses a rather thick and not rectangular structure. Thus, $\widetilde{J}_x(x,y)$ is equivalent to that in a rectangular structure with periodically varying conductivity. To reduce or eliminate the impact of the specimen geometry, a correction factor $C(x,y)$ must be determined from the forward solution provided by the FEM simulation. We used the magnetic field shown in Fig. 1 to compute $\widetilde{J}_x(x_0,y)$ within a homogeneous specimen via deconvolving (4). Fig. 3 shows the resulting $\widetilde{J}_x(x_0,y)$. Since a homogeneous specimen was modeled, the current density $J_x(x_0,y)$ must be constant with $I/A = 12.926\ \mathrm{kA/m^2}$. The ratio of $\widetilde{J}_x(x_0,y)$ and the constant value $J_x(x_0,y)$ determines the correction factor to $C(x_0,y) = J_x(x_0,y)/\widetilde{J}_x(x_0,y)$. The calculated $C(x_0,y)$ models the impact of the triangular geometry and eliminates boundary effects caused by the height of the specimen, since $\mathrm{d}z' = d$ presupposes a thin structure. By multiplying $C(x_0,y)$ with each scan line of the preliminary current density $\widetilde{J}_x(x,y)$ (in Fig. 3) an improved estimate $\widehat{J}_x(x,y)$ can be computed, shown in Fig. 4.

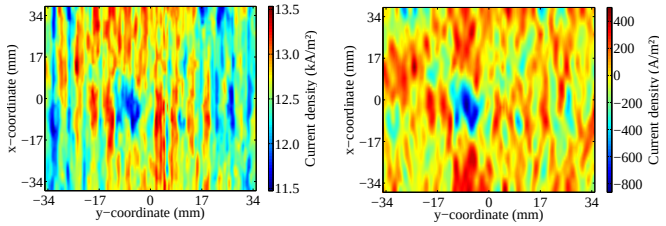

Figure 4. The left image shows the estimated $\widehat{J}_x(x,y)$ obtained from $\widetilde{J}_x(x_0,y)$ with the correction factor $C(x_0,y)$. The right image shows the deviation of $\Delta\widehat{J}_x(x,y)$ within the specimens base area due to variations of the conductivity.

A small inhomogeneity is present at $x = -5\ \mathrm{mm}$ and $y = -14\ \mathrm{mm}$, which is also visible in Fig. 2. At the inhomogeneity, the current is deflected sidewards and into the comb structure. Therefore, strands are partially visible in the region close to the inhomogeneity. To further reduce the influence of the specimen geometry and the measurement setup (e.g. an oblique alignment) linear trends extending in x–direction and the mean value of $\widehat{J}_x(x,y)$ have been removed. The resulting deviation $\Delta\widehat{J}_x(x,y)$ shown in (Fig. 4) indicates changes of the conductivity $\Delta\kappa$ in the specimens base area.

V. Conclusion

We have presented a method to estimate the current density within an inhomogeneous electrically conductive material by measuring the resulting magnetic field. A specimen with an inhomogeneous conductivity and a non–rectangular cross–section was used to demonstrate the method. Finally, conclusions were drawn on the conductivity within the specimen based on the estimated current density distribution.

References

[1] G. Gibson, S. Schultz, T. Carr, and T. Jagielinski, "Spatial mapping of the sensitivity function of magnetic recording heads using a magnetic force microscope as a local flux applicator," *Magnetics, IEEE Transactions on*, vol. 28, 1992.

[2] P. Jansson, *Deconvolution of Images and Spectra: Second Edition*. Dover Publications, New York, 2011.

[3] P. A. Hölzl and B. G. Zagar, "Improving the spatial resolution of magneto resistive sensors via deconvolution," *IEEE Sensors Journal*, submitted for publication.

[4] B. Roth, N. Sepulveda, and J. Wikswo, "Using a magnetometer to image a two-dimensional current distribution," *Journal of applied physics*, 1989.

[5] D. Hofer, T. Wiesner, and B. G. Zagar, "Analyzing 2d current distributions by magnetic field measurements," *2012 IEEE International Instrumentation and Measurement Technology Conference (I2MTC 2012) Proceedings*, 2012.